CCFE
CULHAM CENTRE FOR FUSION ENERGY

UK Atomic Energy Authority

UKAEA-CCFE-CP(20)123

K D Lawson, M Groth, D Harting, S Menmuir, K M Aggarwal, S Brezinsek, I H Coffey, G Corrigan, F P Keenan, C F Maggi, A G Meigs, M G O'Mullane, S Wiesen

Use of the CHEM He II atomic data in JET EDGE2D-EIRENE simulations

Use of the CHEM He II atomic data in JET EDGE2D-EIRENE simulations

K D Lawson, M Groth, D Harting, S Menmuir, K M Aggarwal, S Brezinsek, I H Coffey, G Corrigan, F P Keenan, C F Maggi, A G Meigs, M G O'Mullane, S Wiesen

This paper has been submitted to
24th International Conference on Plasma Surface Interactions in Controlled Fusion Devices (PSI), South Korea, 24 - 29 January 2021

Use of the Culham He Model He II atomic data in JET EDGE2D-EIRENE simulations

K.D. Lawson[1], M. Groth[2], D. Harting[3], S. Menmuir[1], K.M. Aggarwal[4], S. Brezinsek[3], I H Coffey[1,4], G. Corrigan[1], F.P. Keenan[4], C.F. Maggi[1], A.G. Meigs[1], M.G. O'Mullane[5], J. Simpson[1], S. Wiesen[3] & JET Contributors*

EUROfusion Consortium, JET, Culham Science Centre, Abingdon, OX14 3DB, UK

[1]UKAEA/CCFE, Culham Science Centre, Abingdon, OX14 3DB, UK

[2]Aalto University, Otakaari 1, Espoo, 02150, Finland

[3]Forschungszentrum Jülich Gmbh, Institut für Energie- und Klimaforschung – Plasmaphysik, 52425 Jülich, Germany

[4]Astrophysics Research Centre, School of Mathematics and Physics, Queen's University Belfast, Belfast, BT7 1NN, Northern Ireland, UK

[5]Depart. of Physics, University of Strathclyde, Glasgow, G4 0NG, UK

See the author list of E. Joffrin et al., 2019, Nucl. Fusion, **59, 112021*

1. Introduction

Present-day large plasma machines use a divertor containing a cold, dense plasma to act as a buffer between the hot core and the plasma-facing material surfaces, providing protection for the latter. The behaviour of the divertor plasma, including the power radiated by fuel and impurity species, is therefore crucial in determining the performance of the next-step machines such as ITER, requiring transport modelling of the plasma edge and divertor. Transport codes that simulate the edge and divertor plasmas rely on the availability of accurate atomic and molecular data both for the fuel and impurity species. It is important to understand the sensitivity of the simulations to these data, since this determines the quality of the atomic and molecular data required. Recent work has led to the generation of the CHEM (Culham He Model) atomic dataset for hydrogenic He II (He^+) [1,2]. The sensitivity of the simulation codes to the atomic data is being tested by comparing their use in EDGE2D-EIRENE simulations with the presently used data from the ADAS database. Helium is widely used in laboratory fusion experiments both as a fuel as in the first, non-nuclear phase of ITER, as a minority gas for RF heating and will occur as ash from the thermonuclear reactions. The atomic physics of He II is in many ways similar to that of D I, so this study will inform work on D fuelled simulations. We first consider He rather than D, since the former presents a more tractable atomic physics problem in that the heavy particle collisions [1] involve ions rather than neutrals. The use of He simulations also avoids the complications that can result from molecular emissions. This gives a cleaner comparison with experiment, although, in the present study, no attempt is made to compare the simulation results with measurements.

Our study is particularly pertinent in that simulations by Groth *et al*. [3] of L-mode discharges run in JET have consistently shown a shortfall in the radiated power at low temperatures below that measured by bolometry. This applies both to the earlier JET-C campaigns in which the plasma-facing surfaces were predominately C, as well as more recent ones undertaken after the installation in JET of an ITER-like wall (ILW). In JET-ILW, the plasma-facing surfaces in the divertor are W, with a Be wall in the main chamber. Comparisons of EDGE2D-EIRENE simulations with

measured poloidal radiation profiles recorded during JET-ILW, L-mode, D discharges [4] confirm marked differences in the profiles. It is noted that discrepancies are seen at all temperatures. However, at the higher temperatures the lower simulated emission in the inner divertor tends to balance the higher outer divertor simulated emission, reducing the discrepancy in the total radiated power from the divertor. These discrepancies bring into question predictions for the radiated power and cooling of a radiative divertor in a next-step machine. Similar results are found for unseeded ELMy H-mode discharges by Järvinen *et al*. [5] and an analysis of He discharges in DIII-D showing similar features is described by Canik et al. [6].

2. Simulations

D-fuelled EDGE2D-EIRENE simulations [7] were run for a number of densities in which the dominant impurity was He, its density far exceeding that of the D fuel in the plasma. In the high density simulations considered here, the D density in the divertor was typically ~ 4% of that of He. These are the most ITER relevant and a comparison is made between simulations in which the ADAS [8] and CHEM databases are used to provide atomic data for He II, the setup otherwise being the same. EIRENE atomic data are used for D and neutral He (He I).

An important question is whether the CHEM database allows higher densities and lower temperatures to be reached than is possible with the ADAS data, since there is concern that some low temperature extrapolations used in ADAS may limit the temperature range. ADAS '96' data was named for D and both ADAS '89' and '96' datasets were tested for He in standard simulations. Differences were found between these simulations, although crucially the '96' dataset did not allow significantly lower temperatures to be reached, the maximum He impurity content being marginally less than with the '89' dataset. This study will concentrate on quantifying discrepancies with simulations using the CHEM data, the first available comparison being with the ADAS '89' dataset.

The CHEM atomic physics model is described by Lawson *et al*. [1, 2]. The model considers the dominant populating channels for energy levels in a hydrogenic species, including electron and heavy particle collisional excitation and deexcitation, radiative decay, direct electron collisional ionization, radiative and three-body recombination. It can be run as a stand-alone program, with different populating channels readily switched on and off so as to show the importance of their contributions. The database has been adapted into ADAS look-alike datasets so as to allow easy inclusion in the EDGE2D-EIRENE simulations. Crucially, the model makes use of the most recent atomic data, with particular care being taken over any extrapolations required to low temperatures.

EDGE2D uses atomic data for two calculations, one being a post-processing calculation of the radiated power, the second in determining the electron power loss term that is used in the simulation itself. ADAS uses the low-level line power coefficient, PLT, and the recombination-bremsstrahlung power coefficient, PRB, to determine the radiated power, and agreement is found with the CHEM database for this parameter. In addition to the PLT and PRB functions, the electron power loss term depends on the ionization and recombination coefficients, SCD and ACD,

respectively, which give the effective rates at which these processes take place [9]. For hydrogenic species the electron power loss term is given by

$$S_e(z,T_e,n_e) = n_e n_z I_H SCD(z) - n_e n_{z+1} I_H ACD(z+1) + n_e n_z PLT(z) + n_e n_{z+1} PRB(z+1),$$

where z corresponds to the hydrogenic charge state and z+1 that of the fully stripped ion. This term should only include kinetic components, since it is these that affect transport. However, the ACD term does contain a component relating to the potential energy of the system. Significant differences between the two databases are found for the SCD and ACD functions, there being order of magnitude differences at low temperatures [10]. That this could influence the simulations has been shown by Lawson *et al*. [11], who found that by artificially increasing the atomic power loss term in a D simulation in the temperature range 10-30 eV by up to 4% led to a reduction in T_e in some cells of a factor of 10, although it should be noted that this was a worst case.

3. Results

3.1 Comparison of ADAS and CHEM simulations with the same He impurity content

The simulations were run with the same D density control (10^{17} m^{-3}) and He impurity content of 10^{13} particles, these being inputs to the code. They are catalogued under JET pulse 81472, that using ADAS data as '/jul1320/seq#1' and the CHEM data as '/jul1320/seq#2'. It is found that the CHEM simulation has a lower T_e in the outer divertor corner and at the edges of the outer divertor, but with steeper gradients leading up to higher temperatures near the X-point. The corner T_e is ~25% lower at 3.8 eV and that at the outer edges ~10% lower. However, in the CHEM simulation T_e rises to nearly 20 eV close to the divertor compared with ~15 eV in the ADAS case. Comparing electron densities, particles are moved from within the core plasma neighbouring the X-point, into both the inner and outer divertors. In the divertor, the densities are similar close to the X-point, but then increase by up to ~50% in the outer divertor and typically by 25-30% in the inner divertor. Both higher densities and temperatures lead to an increase in radiated power and these are listed in table 1, the contributions being summed for cells below z = -1.43 m, the height of the X-point.

3.2 Comparison of ADAS and CHEM simulations at maximum He impurity content

Using the simulations discussed in section 3.1 as a starting point, the He impurity content was increased until the simulations no longer converged. When the ADAS atomic data was used the highest impurity content achieved was 1.06×10^{13} particles (/jun2820/seq#1), whereas with CHEM data an impurity content of 1.28×10^{13} particles was possible (/jun2820/seq#2). Figures 1 and 2 compare the electron temperatures and electron densities of the simulations, respectively. To better illustrate the changes, T_e is plotted against distance from the divertor plates along field lines (the simulation 'rings') in figure 3. These plots include most of the cells in the inner divertor, but to avoid confusion in the outer divertor plot, a selection of field lines is made, the colour-coded circles in figure 2b indicating the starting point of the field lines at the divertor plates.

As can be seen in figure 2 the trend, noted in section 3.2, of higher n_e is further enhanced. The increase is ×1.5 close to the X-point, but is ~ ×2 throughout most of the outer divertor and somewhat

smaller (×1.65-1.85) in the inner divertor. With the higher densities, T_e (figure 3) is found to be lower, falling to ~2 eV in the outer divertor corner and along the inner divertor plates. This is well below the T_e of 4-5 eV at which the driving channel for populating the lowest He II electronic levels changes from excitation from the ground state to recombination from fully stripped He ions. This is illustrated in figure 4, which shows the radiated power and its various components plotted against T_e. It can be seen that at 5 eV the component in red, which excludes recombination contributions, falls away sharply with decreasing T_e and those components that include recombination increase. Figure 5 shows the ratio of radiated powers from the CHEM and ADAS simulations. The sharp increase in radiation as recombination becomes important can be seen close to the inner divertor plates and in the outermost (red) trace in the outer divertor. Nevertheless, the temperature in most of the divertor region is above ~4 eV and hence the reduction in T_e will lead to lower radiated powers, so that the observed increases are due to the higher densities of the CHEM simulation. The total radiated powers due to He for the two simulations are given in table 2.

4. Conclusions

The shortfall in the simulated divertor radiated power is thought to be due to insufficiently low temperatures being reached in the simulations. This limits the molecular densities achieved in D simulations and consequently the radiation from deuterium molecules. It also prevents the large radiated power expected from recombination-driven populations in atoms from occurring, which is the most likely explanation of the intense, spatially localized features observed close to the inner divertor target plates [3,4]. The simulations using CHEM data allowed low temperatures of ~2 eV to be reached in the outer divertor corner and along the inner divertor plates. Even lower electron temperatures are thought necessary to explain fully the shortfalls in the simulated divertor radiated power. This analysis demonstrates the need for the highest quality atomic data to be used in order to give the reliable edge transport simulations.

This work has been carried out within the framework of the EUROfusion Consortium and has received funding from the Euratom research and training programme 2014-2018 and 2019-2020 under grant agreement No 633053 and from the RCUK, grant number EP/T012250/1. The views and opinions expressed herein do not necessarily reflect those of the European Commission.

References

[1] K D Lawson *et al*., 2019, J. Phys. B, **52**, 045001
[2] K D Lawson *et al*., 2020, To be submitted to J.Phys. B
[3] M Groth *et al*., 2013, Nuc. Fus., **53**, 093016.
[4] K D Lawson *et al.,* 2013, Proc. 40th EPS Conf., Espoo, Finland
[5] A Järvinen *et al*., 2015, JNM, **463**, 135
[6] Canik *et al*., 2017, Phys. of Plas., **24**, 056116
[7] S Wiesen, 2006, http://www.eirene.de/e2deir_report_30jun06.pdf
[8] H P Summers, 2004, 'The ADAS User Manual, version 2.6, http://adas.phys.strath.ac.uk'
[9] H P Summers *et al*., 2006, PPCF, **48**, 263.
[10] K D Lawson *et al.,* 2019, Proc. 46th EPS Conf., Milan
[11] K D Lawson *et al.,* 2018, Proc. 45th EPS Conf., Prague

Table 1. He divertor radiated powers (W) from simulations using ADAS and CHEM He II atomic databases at the same impurity content

	Inner divertor radiated power (W)			Outer divertor radiated power (W)		
	'89' ADAS	CHEM	Ratio	'89' ADAS	CHEM	Ratio
He I	5.23e+3	7.81e+3	1.49	2.25e+4	2.70e+4	1.20
He II	1.59e+4	2.46e+4	1.55	4.70e+4	5.92e+4	1.26
Total	2.11e+4	3.25e+4	1.54	6.95e+4	8.62e+4	1.24

Table 2. He divertor radiated powers (W) from simulations using ADAS and CHEM He II atomic databases at maximum impurity content

	Inner divertor radiated power (W)			Outer divertor radiated power (W)		
	'89' ADAS	CHEM	Ratio	'89' ADAS	'96' ADAS	Ratio
He I	3.53e+3	5.45e+3	1.54	1.76e+4	2.08e+4	1.18
He II	6.44e+3	9.42e+3	1.46	2.67e+4	2.79e+4	1.04
Total	9.96e+4	1.49e+4	1.50	4.43e+4	4.87e+4	1.10

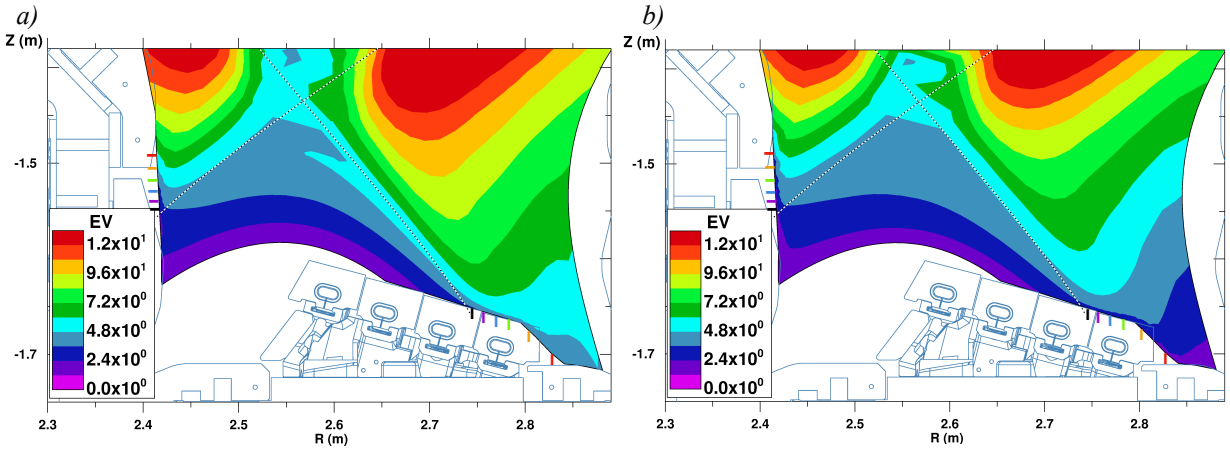

Figure 1. Electron temperatures from simulations with maximum impurity content that use a) ADAS, b) CHEM He II atomic data. Coloured marker lines indicate beginning of field lines used in figures 3 and 5.

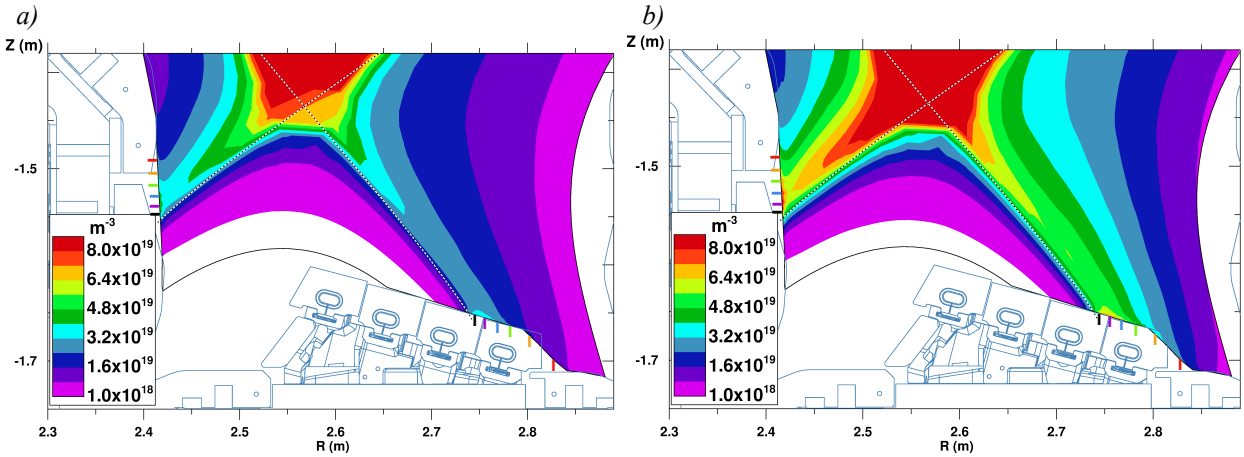

Figure 2. Electron densities from simulations with maximum impurity content that use a) ADAS, b) CHEM He II atomic data. Coloured marker lines indicate beginning of field lines used in figure 3 and 5.

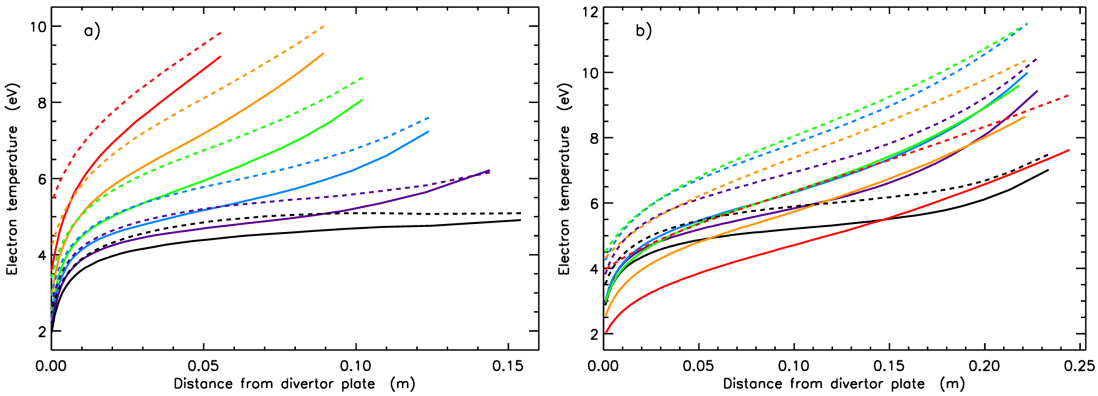

Figure 3. Simulated electron temperatures along field lines for a) the inner divertor and b) the outer divertor: full lines CHEM database, dotted lines ADAS database. The coloured marker lines in figures 1 and 2 show the starting point of the field lines at the divertor plates.

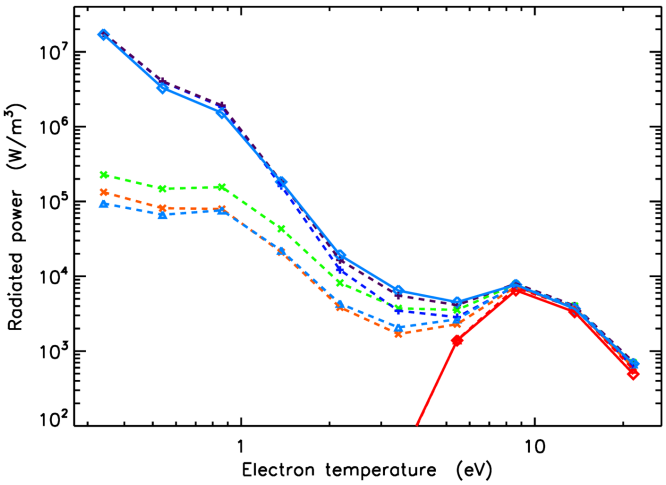

Figure 4. Radiated power as a function of T_e given by the ADAS He II PLT and PLT+PRB functions (full lines) compared with He II radiated powers found using CHEM (dashed lines). The data apply to a ring of cells from a simulation in which the temperature varies from 0.29 to 21.2 eV. Various processes are included in the model:- full model, without 3-body recombination rates and without 3-body and radiative recombination rates, and the corresponding curves excluding radiation directly from radiative recombination; full model, without 3-body recombination rates and without 3-body and radiative recombination rates, the latter essentially including no recombination effects and hence corresponding to the ADAS PLT function

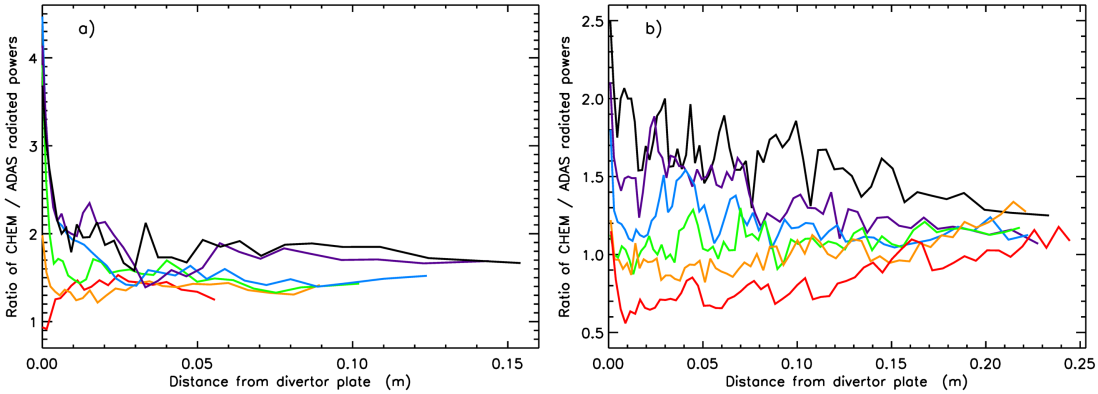

Figure 5. Ratio of the CHEM to ADAS simulated radiated powers along field lines for a) the inner divertor and b) the outer divertor. The coloured marker lines in figure 2 show the starting point of the field lines at the divertor plates.